Journal of Statistical Physics, Vol. 42, Nos. 3/4, 1986

The Ground States of the Classical Heisenberg and Planar Models on the Triangular and Plane Hexagonal Lattices

Shigetoshi Katsura,[1] Tsugio Ide,[1] and Tohru Morita[2]

Received March 4, 1985

The energies and the spin configurations of the ground states of the classical Heisenberg and classical planar (XY) models with first- and second-neighbor interactions on the triangular and plane hexagonal lattices are obtained. The phase diagrams in the J_1–J_2 plane are determined, where J_1 and J_2 are the coefficients of the first- and second-neighbor interactions, respectively. It is noted for the system on the plane hexagonal lattice, that an infinite degeneracy of the ground states occurs in some region of the J_1–J_2 plane and then the study is made under an introduction of an infinitesimal third-neighbor interaction, removing the degeneracy.

KEY WORDS: Heisenberg model; planar model; XY model; triangular lattice; hexagonal lattice; ground state.

1. INTRODUCTION

Recently magnetic properties of low-dimensional substances have received much attention. In particular, substances on the triangular and hexagonal lattices attracted much interest owing to the variety of the phases. The ground states of the Ising models with first- and second-neighbor interactions were determined by Kaburagi and Kanamori[1] for the systems on the triangular lattice and by Kudō and Katsura[2] for those on the hexagonal close-packed and plane hexagonal lattices. The ground states of the classical Heisenberg model were investigated for the systems on the bcc, fcc, and other lattices by Yoshimori,[3] Lyons and Kaplan,[4] and Nagamiya,[5] and his group.[6]

[1] Department of Applied Physics, Tohoku University, Sendai, Japan.
[2] Department of Engineering Science, Tohoku University, Sendai, Japan.

0022-4715/86/0200-0381$05.00/0

The systems on the triangular and plane hexagonal lattices, however, have not been investigated so far in detail. In this paper the ground states of the classical Heisenberg and planar (XY) models on the both lattices are obtained. The coefficients of the first- and second-neighbor interactions are denoted by J_1 and J_2, respectively.[3] The J_1–J_2 plane is divided into regions in which various phases, including the triangular and helical phases, occur, and the spin configurations in the respective regions are determined. For the system on the plane hexagonal lattice, the ground state is degenerate infinitely in some region of the plane, and a third-neighbor interaction is included to remove it.

In Sections 2 and 3, the systems on the triangular and plane hexagonal lattices, respectively, are studied. Section 4 is for conclusion and discussion.

2. TRIANGULAR LATTICE

We consider the classical Heisenberg and planar (XY) models with first- and second-neighbor interactions, on the triangular lattice. We use the oblique coordinate system shown in Fig. 1. A unit cell contains one spin. The position of a spin m is denoted by $\mathbf{R}_m$. Let the exchange energy between spins m and n be $-2J_{mn}\mathbf{S}_m \cdot \mathbf{S}_n$. Here $\mathbf{S}_m$ is a classical unit vector in d dimensions, such that

$$\mathbf{S}_m \cdot \mathbf{S}_m = 1 \tag{2.1}$$

We assume $d=2$ or 3. The coefficient J_{mn} is set equal to J_1 and J_2 when m and n are first and second neighbors, respectively, and zero otherwise. $\{J_{mn}\}$ satisfy $J_{mn}=J_{nm}=J_{m-n,0}$ (translational invariance). The Hamiltonian of the system is expressed as follows:

$$\mathscr{H} = -\sum_m \sum_n J_{mn}\mathbf{S}_m \cdot \mathbf{S}_n \tag{2.2}$$

When $d=3$, the Hamiltonian is the one for the classical Heisenberg model, and when $d=2$ it is the one for the planar (XY) model.

Let

$$\boldsymbol{\sigma}_{\mathbf{q}} \equiv \frac{1}{N}\sum_m \mathbf{S}_m \exp(-i\mathbf{q}\cdot\mathbf{R}_m), \qquad \boldsymbol{\sigma}_{\mathbf{q}}^* = \boldsymbol{\sigma}_{-\mathbf{q}} \tag{2.3a}$$

$$\tilde{J}(\mathbf{q}) \equiv \sum_m J_{mn} \exp(i\mathbf{q}\cdot\mathbf{R}_{mn}) \tag{2.3b}$$

[3] The antiferromagnetic classical XY model with first-neighbor interaction is treated in Ref. 7.

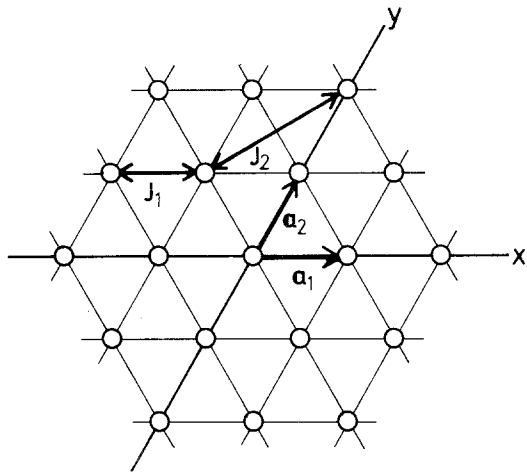

Fig. 1. Oblique coordinate system of the triangular lattice employed in the present paper.

so that

$$\mathbf{S}_m = \sum_{\mathbf{q}} \boldsymbol{\sigma}_{\mathbf{q}} \exp(i\mathbf{q} \cdot \mathbf{R}_m) \tag{2.4a}$$

$$J_{mn} = \frac{1}{N} \sum_{\mathbf{q}} \tilde{J}(\mathbf{q}) \exp(-i\mathbf{q} \cdot \mathbf{R}_{mn}) \tag{2.4b}$$

where $\mathbf{R}_{mn} \equiv \mathbf{R}_m - \mathbf{R}_n$, and $\mathbf{q}$ are those wave vectors in the first Brillouin zone that $\exp(i\mathbf{q} \cdot \mathbf{R})$ obeys the periodic boundary condition, and N is the total number of unit cells in the system. By using (2.3a) and (2.3b), Eqs. (2.2) and (2.1) are transformed into

$$\mathscr{H} = -N \sum_{\mathbf{q}} \tilde{J}(\mathbf{q})\, \boldsymbol{\sigma}_{\mathbf{q}} \cdot \boldsymbol{\sigma}_{\mathbf{q}}^* \tag{2.5}$$

$$\sum_{\mathbf{q}} \boldsymbol{\sigma}_{\mathbf{q}} \cdot \boldsymbol{\sigma}_{\mathbf{q}-\mathbf{q}'}^* = \delta_{\mathbf{q}',0} \tag{2.6}$$

Our problem is to find $\{\mathbf{S}_m\}$ which makes $\mathscr{H}$ given by (2.2) minimum under the strong constraint (2.1), that is, equivalent to find $\{\boldsymbol{\sigma}_{\mathbf{q}}\}$ which makes $\mathscr{H}$ given by (2.5) minimum under the constraint (2.6). We, however, look for the minimum of $\mathscr{H}$ under the weak constraint

$$\sum_{\mathbf{q}} \boldsymbol{\sigma}_{\mathbf{q}} \cdot \boldsymbol{\sigma}_{\mathbf{q}}^* = 1 \tag{2.7}$$

that is, we require (2.6) only for $\mathbf{q}'=0$, which is equivalent to one condition $\sum_m \mathbf{S}_m \cdot \mathbf{S}_m = N$ in place of N conditions in (2.1). If the obtained $\{\mathbf{S}_m\}$ satisfies the strong constraint (2.2), the spin configuration is one of those which give the minimum of $\mathscr{H}$ under the strong constraint.[4]

We take variations of $\mathscr{H}$ given by (2.5) with respect to $\boldsymbol{\sigma}_{\mathbf{q}}^*$ under the subsidiary condition (2.7). By using the Lagrangian multiplier λ, we have

$$\sum_{\mathbf{q}} [\tilde{J}(\mathbf{q})\,\boldsymbol{\sigma}_{\mathbf{q}} - \lambda \boldsymbol{\sigma}_{\mathbf{q}}] \cdot \delta\sigma_{\mathbf{q}}^* = 0$$

This condition leads to $\lambda = \tilde{J}(\mathbf{q})$ or $\boldsymbol{\sigma}_{\mathbf{q}} = 0$. This means that when $\lambda = \tilde{J}(\mathbf{q}_1)$ for some $\mathbf{q}_1$, then $\boldsymbol{\sigma}_{\mathbf{q}_2} = 0$ for all $\mathbf{q}_2$ for which $\tilde{J}(\mathbf{q}_2) \neq \tilde{J}(\mathbf{q}_1)$. Now we have

$$\varepsilon \equiv \mathscr{H}/N = -\tilde{J}(\mathbf{q}_1) \tag{2.8}$$

and the $\{\mathbf{S}_m\}$ is given by (2.4a) in terms of $\boldsymbol{\sigma}_{\mathbf{q}}$, which are nonzero only for those $\mathbf{q}$ satisfying $\tilde{J}(\mathbf{q}) = \tilde{J}(\mathbf{q}_1)$, and these nonzero values of $\boldsymbol{\sigma}_{\mathbf{q}}$ are only restricted by the condition (2.7).

Now we look for a $\mathbf{q}_1$ which makes (2.8) minimum. Let $q_x = \mathbf{q} \cdot \mathbf{a}_1$ and $q_y = \mathbf{q} \cdot \mathbf{a}_2$, where $\mathbf{a}_1$ and $\mathbf{a}_2$ are the unit vectors in the oblique coordinate system as shown in Fig. 1. Then

$$\begin{aligned}\tilde{J}(\mathbf{q}) &= 2J_1[\cos q_x + \cos q_y + \cos(q_x - q_y)] \\ &\quad + 2J_2[\cos(q_x + q_y) + \cos(2q_x - q_y) + \cos(q_x - 2q_y)] \qquad (2.9) \\ &= 2J_1(2XY + 2Y^2 - 1) + 2J_2[2X^2 - 1 + 2XY(4Y^2 - 3)] \qquad (2.10)\end{aligned}$$

where

$$X \equiv \cos\frac{q_x + q_y}{2}, \qquad Y \equiv \cos\frac{q_x - q_y}{2} \tag{2.11}$$

The expression (2.10) can be written as follows:

$$\begin{aligned}\tilde{J}(\mathbf{q}) = 2J_1 &\left\{\cos[q\cos\phi] + \cos\left[q\cos\left(\phi - \frac{2\pi}{3}\right)\right]\right. \\ &\left. + \cos\left[q\cos\left(\phi - \frac{4\pi}{3}\right)\right]\right\} \\ + 2J_2 &\left\{\cos\left[\sqrt{3}\,q\cos\left(\phi - \frac{\pi}{6}\right)\right] + \cos\left[\sqrt{3}\,q\cos\left(\phi - \frac{5\pi}{6}\right)\right]\right. \\ &\left. + \cos\left[\sqrt{3}\,q\cos\left(\phi - \frac{9\pi}{6}\right)\right]\right\} \qquad (2.12)\end{aligned}$$

where $q = |\mathbf{q}|$ and ϕ is the azimuthal angle of $\mathbf{q}$ in the polar coordinate system. The sixfold symmetry of $\tilde{J}(\mathbf{q})$ is observed in this expression (2.12).

The conditions $\partial\tilde{J}(\mathbf{q})/\partial q_x = \partial\tilde{J}(\mathbf{q})/\partial q_y = 0$ give

$$[J_1 Y + J_2(2X + 4Y^3 - 3Y)](1 - X^2)^{1/2} = 0 \tag{2.13}$$

$$[J_1(X + 2Y) + J_2(12XY^2 - 3X)](1 - Y^2)^{1/2} = 0 \tag{2.14}$$

The solutions under the weak constraint are determined by (2.13) and (2.14), and they are classified in five types, F (ferromagnetic), AF (antiferromagnetic), T (triangular), H_1 (helical) and H_2 (helical), in Table I, which are candidates of the ground state. Figure 2 shows the value of ε/J_2 as a function of $\xi \equiv J_1/J_2$. We see that H_2 does not appear as a ground state. The $\mathbf{q}$ for the other four types of states are shown in Fig. 3 in

Table I. Spin Configurations of the Systems on the Triangular Lattice, and the Wave Number $\mathbf{q} = (q_x, q_y)$ and the Energy.[a]

Type	$\cos Q_1 = -\frac{1}{2}(\xi+1)$, (X, Y)	$\cos Q_2 = \frac{1}{2} - \frac{\xi}{6}$, (q_x, q_y)	$\xi \equiv \frac{J_1}{J_2}$ Energy per unit cell
F	$(\pm 1, \pm 1)$	$(0, 0)$	$-6J_2(\xi+1)$
AF	$(\pm 1, \mp 1)$	(π, π)	$2J_2(\xi+1)$
	$(0, 0)$	$(\pi, 0)$	
		$(0, \pi)$	
T	$\left(\pm 1, \mp\frac{1}{2}\right)$	$\left(\pm\frac{2}{3}\pi, \mp\frac{2}{3}\pi\right)$	$3J_2(\xi-2)$
H_1	$\left(\mp\frac{1}{2}(\xi+1), \pm 1\right)$	(Q_1, Q_1)	$J_2(\xi^2+3)$
	$\left(\pm\frac{1}{2}(1-\xi)^{1/2}, \pm\frac{1}{2}(1-\xi)^{1/2}\right)$	$(Q_1, 0)$	$(-3 \leqslant \xi \leqslant 1)$
		$(0, Q_1)$	
H_2	$\left(\pm 1, \pm\left(\frac{1}{2} - \frac{\xi}{6}\right)\right)$	$(Q_2, -Q_2)$	$J_2(-\xi^3 + 18\xi^2 - 27\xi + 54)/27$
	$\left(\pm\frac{\xi}{6}\left(3 - \frac{\xi}{3}\right)^{1/2}, \mp\frac{1}{2}\left(3 - \frac{\xi}{3}\right)^{1/2}\right)$	$(2Q_2, Q_2)$	$(-3 \leqslant \xi \leqslant 9)$
		$(Q_2, 2Q_2)$	

[a] Double signs refer the same order. Q_1 and Q_2 are taken such that $\mathbf{q}$ lies in the first Brillouin zone.

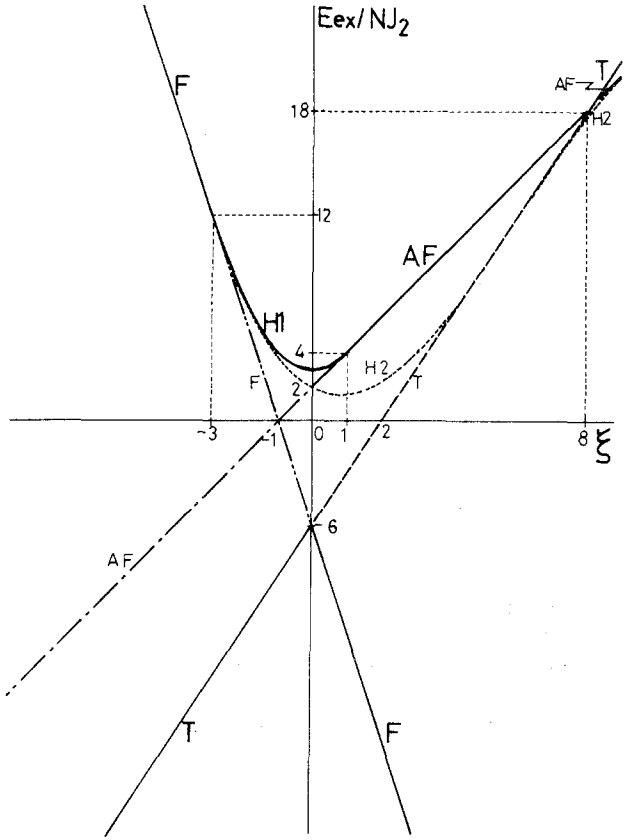

Fig. 2. ε/J_2 versus ξ for several states of the systems on the triangular lattice. Here E_{ex}/N denotes ε, and $\xi = J_1/J_2$.

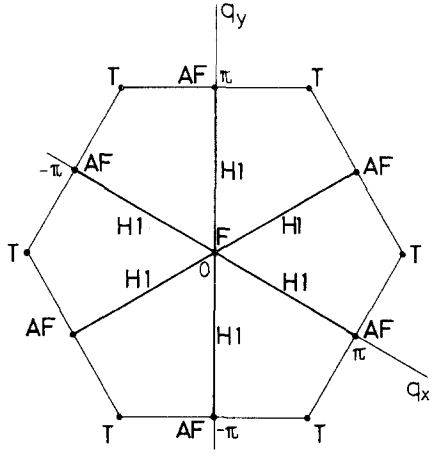

Fig. 3. The first Brillouin zone of the triangular lattice. F, AF, T, and H_1 are the spin configurations in the ground states. The lines connecting the origin and T are H_2, which are not realized as a ground state.

the first Brillouin zone. All these states except F have the sixfold symmetry as we can see in (2.12).

In the ferromagnetic state F where $\mathbf{q}=0$, the spin configuration is given by

$$\mathbf{S}_m = \mathbf{u} \tag{2.15}$$

where $\mathbf{u}$ is a unit vector in any direction. (2.15) satisfies the strong constraint (2.1).

In the antiferromagnetic state AF, $\tilde{J}(\mathbf{q})$ is degenerate for $\mathbf{q}=\mathbf{q}_i$, for $i=1$, 2, and 3, where $\mathbf{q}_1=(\pi, \pi)$, $\mathbf{q}_2=(\pi, 0)$, and $\mathbf{q}_3=(0, \pi)$. The general solution under the weak constraint is given by

$$\mathbf{S}_n = \sum_{l=1}^{3} \mathbf{b}_l \exp(i\mathbf{q}_l \cdot \mathbf{R}_n) \tag{2.16}$$

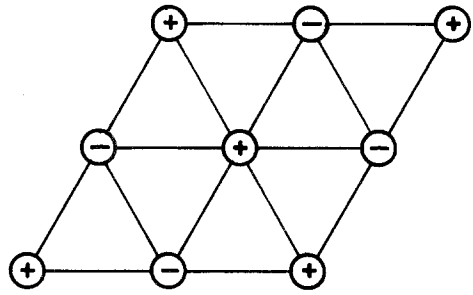

(a)

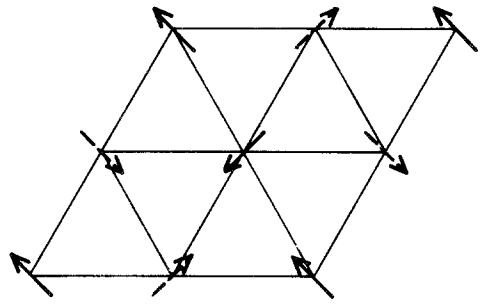

(b)

Fig. 4. Spin configurations of the systems on the triangular lattice in the antiferromagnetic state. (a) $\mathbf{q}=(\pi, \pi)$; the $\mathbf{u}_\mathbf{q}$–$\mathbf{v}_\mathbf{q}$ plane coincides with the x–z plane. + and − indicate that the spin directs upward and downward, respectively. (b) Example where the $\mathbf{u}_\mathbf{q}$–$\mathbf{v}_\mathbf{q}$ plane is oblique to the x–z plane. The arrows show the projection on the x–y plane. The solid and dashed arrows mean that the z components are positive and negative, respectively.

where $\{\mathbf{b}_l\}$ is an arbitrary set of three vectors satisfying

$$\mathbf{b}_1 \cdot \mathbf{b}_1 + \mathbf{b}_2 \cdot \mathbf{b}_2 + \mathbf{b}_3 \cdot \mathbf{b}_3 = 1 \tag{2.17}$$

If we further require

$$\mathbf{b}_l \cdot \mathbf{b}_{l'} = 0 \qquad (l \neq l') \tag{2.18}$$

the solution satisfies also the strong constraint (2.1); we can easily see that (2.18) is also necessary for this. Then $\mathbf{b}_1$, $\mathbf{b}_2$, and $\mathbf{b}_3$ are three mutually orthogonal vectors, and the length of their sum is unity. Figure 4 shows the cases of (a) $\mathbf{b}_1 = \mathbf{b}_2 = 0$, $\mathbf{b}_3 = \mathbf{k}$ and (b) $\mathbf{b}_1 = \mathbf{i}/\sqrt{3}$, $\mathbf{b}_2 = \mathbf{j}/\sqrt{3}$, $\mathbf{b}_3 = \mathbf{k}/\sqrt{3}$, where $\mathbf{i}$, $\mathbf{j}$, and $\mathbf{k}$ are the unit vectors in the x, y, and z directions, respectively.

Let the spin configuration in the state H_1 be

$$\mathbf{S}_n = \sum_{l=1}^{3} \mathbf{b}_l \exp(i\mathbf{q}_l \cdot \mathbf{R}_n) + \sum_{l=1}^{3} \mathbf{b}_l^* \exp(-i\mathbf{q}_l \cdot \mathbf{R}_n) \tag{2.19}$$

where $\mathbf{q}_1 = (Q_1, Q_1)$, $\mathbf{q}_2 = (Q_1, 0)$, and $\mathbf{q}_3 = (0, Q_1)$, and Q_1 is given in Table I. The weak constraint requires

$$\sum_{l=1}^{3} \mathbf{b}_l \cdot \mathbf{b}_l^* = 1/2$$

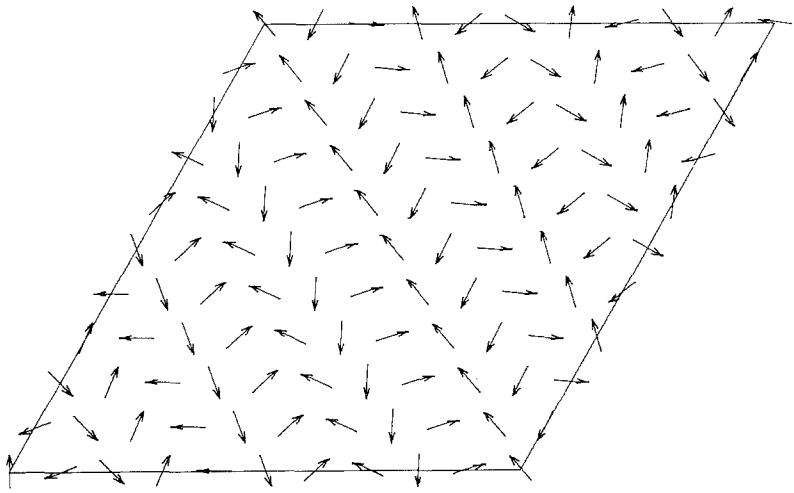

Fig. 5. Helical ordering H_1 of the systems on the triangular lattice; $J_1/J_2 = -1/4$ and $\mathbf{q} = (0.622\pi, 0.622\pi)$.

The strong constraint (2.1) now gives

$$\mathbf{b}_l \cdot \mathbf{b}_{l'} = 0, \qquad \mathbf{b}_l^* \cdot \mathbf{b}_{l'}^* = 0 \qquad (l, l' = 1, 2, 3)$$
$$\mathbf{b}_l \cdot \mathbf{b}_{l'}^* = 0 \qquad (l, l' = 1, 2, 3; l \neq l') \tag{2.20}$$

The conditions (2.20) require that two among $\mathbf{b}_1$, $\mathbf{b}_2$, and $\mathbf{b}_3$ are zero and only one (say $\mathbf{b}_1$) is given by

$$\mathbf{b}_1 = \tfrac{1}{2}(\mathbf{u}_\mathbf{q} - i\mathbf{v}_\mathbf{q}) \tag{2.21}$$

where $\mathbf{u}_\mathbf{q}$ and $\mathbf{v}_\mathbf{q}$ are an arbitrary set of orthogonal unit vectors. Hence

$$\mathbf{S}_n = \mathbf{u}_\mathbf{q} \cos(\mathbf{q} \cdot \mathbf{R}_n) + \mathbf{v}_\mathbf{q} \sin(\mathbf{q} \cdot \mathbf{R}_n) \tag{2.22}$$

The state H_1 is a helical state and the spin configuration is shown in Fig. 5.

In the state T, $\{\mathbf{S}_n\}$ is given also by (2.22) if we put $\mathbf{q}$ equal to either one of $\pm(2\pi/3, -2\pi/3)$. Then the lattice points are divided into three sublattices: α, $(m, m+3p)$; β, $(m, m+3p+1)$; and γ, $(m, m+3p+2)$, and we have $\mathbf{S}_n = \mathbf{u}_\mathbf{q}$, $(-\mathbf{u}_\mathbf{q} \mp \sqrt{3}\,\mathbf{v}_\mathbf{q})/2$, and $(-\mathbf{u}_\mathbf{q} \pm \sqrt{3}\,\mathbf{v}_\mathbf{q})/2$ for the α, β, and γ sublattices, respectively. The double signs here correspond to those of $\mathbf{q}$. The state T is a triangular state and is shown in Fig. 6. The phase diagram in the $J_1 - J_2$ plane is shown in Fig. 7. It is compared with that of the corresponding Ising model[1] shown in Fig. 8. The change of the wave vector against the ratio of the exchange interactions ξ, is shown in Fig. 9. As J_1 decreases from plus infinity to minus infinity for a fixed negative J_2, a component of the wave vector $\mathbf{q}$ changes as $0 \to Q_1 \to \pi \to 2\pi/3$, which correspond to the change of states $F \to H_1 \to AF \to T$, where Q_1 is given in Table I. The first and second transitions are of the second order, while the third one is of the first order.

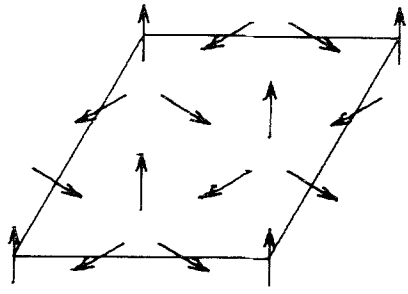

Fig. 6. State T of the systems on the triangular lattice; $\mathbf{q} = [(2/3)\pi, -(2/3)\pi]$.

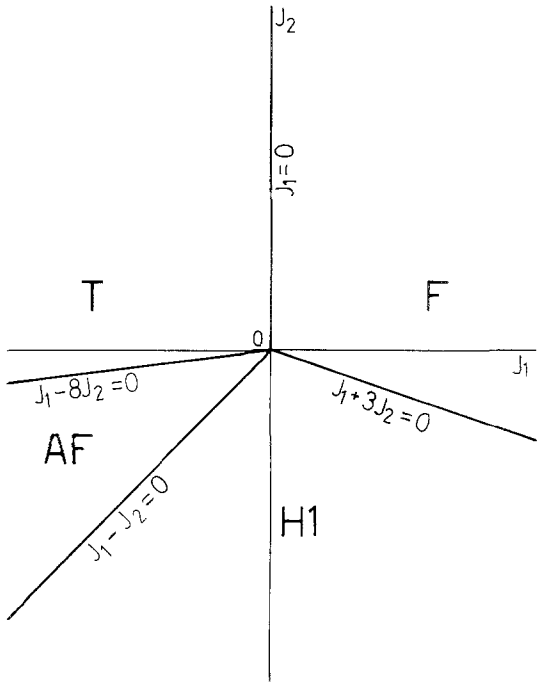

Fig. 7. Phase diagram of the classical Heisenberg and planar models on the triangular lattice in the J_1–J_2 plane.

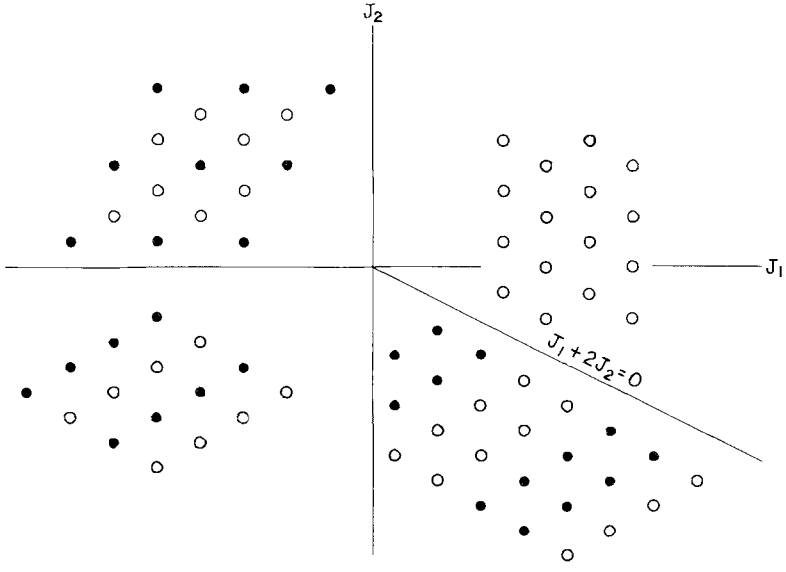

Fig. 8. Phase diagram of the Ising model on the triangular lattice in the J_1–J_2 plane.

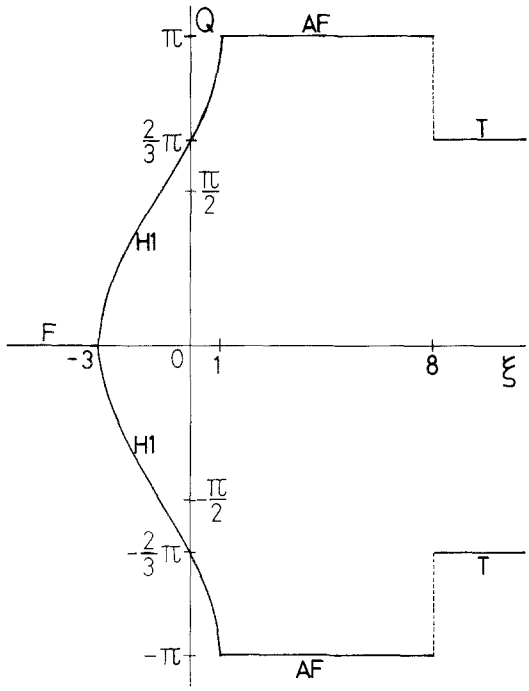

Fig. 9. A component Q of $\mathbf{q}$ versus ξ, showing the change of the wave vector $\mathbf{q}$ against the ratio of the exchange interactions of the systems on the triangular lattice.

The chirality $\boldsymbol{\kappa}$ is defined by[8,9]

$$\boldsymbol{\kappa} \equiv \frac{2}{3\sqrt{3}} (\mathbf{S}_\beta \times \mathbf{S}_\alpha + \mathbf{S}_\gamma \times \mathbf{S}_\beta + \mathbf{S}_\alpha \times \mathbf{S}_\gamma)$$

This is shown to be equal to $\pm \mathbf{w}_\mathbf{q} \equiv \pm \mathbf{u}_\mathbf{q} \times \mathbf{v}_\mathbf{q}$ ($\mathbf{w}_\mathbf{q}$ is the unit vector perpendicular to the $\mathbf{u}_\mathbf{q}$–$\mathbf{v}_\mathbf{q}$ plane in the right-hand system). In general, $\mathbf{u}_\mathbf{q}$ and $\mathbf{v}_\mathbf{q}$ have z components in the classical Heisenberg model. If we restrict $\mathbf{u}_\mathbf{q}$ and $\mathbf{v}_\mathbf{q}$ in the x–y plane, we get ground states of the classical planar model. In this case $\boldsymbol{\kappa} = \mathbf{k}$ or $-\mathbf{k}$, one of the two choices, and $\boldsymbol{\kappa}$ can be regarded as an order parameter.[8,9] In Figs. 5 and 6, arrows are to be understood as drawn not in the x–y plane but in the $\mathbf{u}_\mathbf{q}$–$\mathbf{v}_\mathbf{q}$ plane associated to each lattice point, in the case of the classical Heisenberg model.

3. PLANE HEXAGONAL LATTICE

We consider the classical Heisenberg and planar (XY) models on the plane hexagonal lattice. We take an oblique coordinate system as shown in

Fig. 10. A unit cell contains two spins. The coefficients of the interactions are denoted by $-2J_1$, $-2J_2$, and $-2J_3$, between first, second, and third neighbors, respectively. We include third-neighbor interactions, since the ground state of the system only with the first- and second-neighbor interactions is degenerate infinitely in some cases, as will be seen later. Let the spin vector of the νth atom ($\nu = 1, 2$) in the nth unit cell be $\mathbf{S}_{n\nu}$ and its position be $\mathbf{R}_{n\nu} = \mathbf{R}_n + \mathbf{R}_\nu$, where $\mathbf{R}_n$ is the translational lattice vector. The lattice distance between second neighbors is taken as a unit of length.

The Hamiltonian $\mathscr{H}$ is written as

$$\mathscr{H} = -\sum_m \sum_n \sum_\mu \sum_\nu J_{m\mu,n\nu} \mathbf{S}_{m\mu} \cdot \mathbf{S}_{n\nu} \tag{3.1}$$

$$= -N \sum_{\mathbf{q}} \sum_\mu \sum_\nu \tilde{J}_{\mu\nu}(\mathbf{q})\, \sigma_{\mathbf{q}\mu} \cdot \sigma^*_{\mathbf{q}\nu} \tag{3.2}$$

where N is the total number of unit cells, and

$$\sigma_{\mathbf{q}\mu} = \sigma^*_{-\mathbf{q}\mu} = \frac{1}{N} \sum_m \mathbf{S}_{m\mu} \exp(-i\mathbf{q} \cdot \boldsymbol{R}_{m\mu}) \tag{3.3}$$

$$\tilde{J}_{\mu\nu}(\mathbf{q}) = \sum_m J_{m\mu,n\nu} \exp[i\mathbf{q} \cdot (\mathbf{R}_{m\mu} - \mathbf{R}_{n\nu})] \tag{3.4}$$

The strong constraint in the present problem is given by

$$\mathbf{S}_{m\mu} \cdot \mathbf{S}_{m\mu} = 1 \tag{3.5a}$$

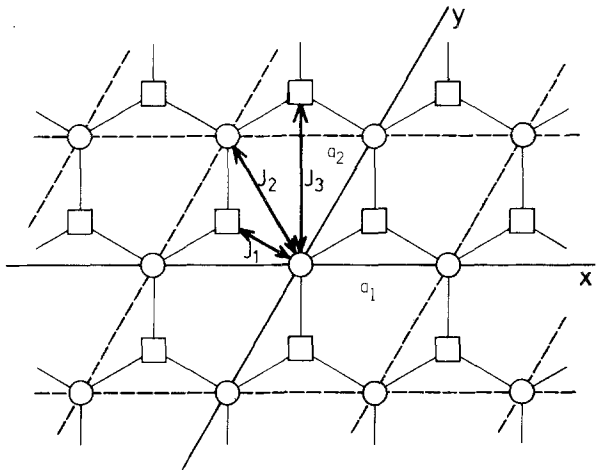

Fig. 10. Oblique coordinate system on the plane hexagonal lattice employed in the present paper. Circles and squares denote the sites on the sublattices $\nu = 1$ and 2, respectively.

that is,

$$\sum_{\mathbf{q}} \boldsymbol{\sigma}_{\mathbf{q}\mu} \cdot \boldsymbol{\sigma}^*_{\mathbf{q}-\mathbf{q}',\mu} = \delta_{\mathbf{q}',0} \tag{3.5b}$$

As the weak constraint, we use

$$\sum_{\mathbf{q}} \sum_{\mu} \boldsymbol{\sigma}_{\mathbf{q}\mu} \cdot \boldsymbol{\sigma}^*_{\mathbf{q}\mu} = 2 \tag{3.6}$$

which is a sum of (3.5b) for $\mathbf{q}' = 0$, and is equivalent to

$$\sum_{m} \sum_{\mu} \mathbf{S}_{m\mu} \cdot \mathbf{S}_{m\mu} = 2N$$

We take variations of $\mathscr{H}$ given by (3.2) with respect to $\boldsymbol{\sigma}^*_{\mathbf{q}\nu}$, under the weak constraint (3.6). By using the Lagrange multiplier λ, we have

$$\sum_{\nu} \sum_{\mathbf{q}} \sum_{\mu} [\tilde{J}_{\mu\nu}(\mathbf{q})\, \boldsymbol{\sigma}_{\mathbf{q}\mu} - \lambda \boldsymbol{\sigma}_{\mathbf{q}\nu}] \cdot \delta \boldsymbol{\sigma}^*_{\mathbf{q}\nu} = 0$$

The minimum of the energy is realized when

$$\sum_{\mu} [\tilde{J}_{\mu\nu}(\mathbf{q}) - \lambda \delta_{\mu\nu}]\, \boldsymbol{\sigma}_{\mathbf{q}\mu} = 0 \tag{3.7}$$

Hence if $\boldsymbol{\sigma}_{\mathbf{q}\mu}$ is nonzero for a certain $\mathbf{q} = \mathbf{q}_1$, λ must be equal to one of the eigenvalues $\lambda_1^{(\pm)}(\mathbf{q}_1)$ of the 2×2 matrix $(\tilde{J}_{\mu\nu}(\mathbf{q}_1))$, and $\sigma_{\mathbf{q}\mu} = 0$ for $\mathbf{q} = \mathbf{q}_2$ if both of the eigenvalues $\lambda^{(\pm)}(\mathbf{q}_2)$ of the matrix $(\tilde{J}_{\mu\nu}(\mathbf{q}_2))$ are not equal to twice the λ, and $\mathscr{H}/N$ is equal to negative twice the λ. Thus, $-\varepsilon = -\mathscr{H}/N$ is equal to twice of one of the eigenvalues $\lambda^{(\pm)}(\mathbf{q})$ of the matrix $(\tilde{J}_{\mu\nu}(\mathbf{q}))$ for a $\mathbf{q}$ and the spin configuration is given by a linear combination of those eigenvectors $\boldsymbol{\sigma}^{(\pm)}_{\mathbf{q}\nu}$ that the corresponding eigenvalues are equal to half of the $-\varepsilon$. Since $\tilde{J}_{11}(\mathbf{q}) = \tilde{J}_{22}(\mathbf{q})$ and $\tilde{J}_{12}(\mathbf{q}) = \tilde{J}^*_{21}(\mathbf{q})$, the normalized eigenvectors and eigenvalues are given by

$$\begin{pmatrix} \boldsymbol{\sigma}^{(\pm)}_{\mathbf{q}1} \\ \boldsymbol{\sigma}^{(\pm)}_{\mathbf{q}2} \end{pmatrix} = \frac{1}{\sqrt{2}} \begin{pmatrix} 1 \\ \pm e^{i\alpha'} \end{pmatrix} \mathbf{u} \tag{3.8}$$

and

$$\begin{aligned} \lambda^{(\pm)}(\mathbf{q}) &= \sum_{\mu} \sum_{\nu} \tilde{J}_{\mu\nu}(\mathbf{q})\, \boldsymbol{\sigma}^{(\pm)}_{\mathbf{q}\mu} \cdot \boldsymbol{\sigma}^{(\pm)*}_{\mathbf{q}\nu} \\ &= \frac{1}{2} (1 \pm e^{i\alpha'}) \begin{pmatrix} \tilde{J}_{11}(\mathbf{q}) & J_1 A e^{i\alpha'} \\ J_1 A e^{-i\alpha'} & \tilde{J}_{11}(\mathbf{q}) \end{pmatrix} \begin{pmatrix} 1 \\ \pm e^{-i\alpha'} \end{pmatrix} \\ &= \tilde{J}_{11}(\mathbf{q}) \pm J_1 A \end{aligned} \tag{3.9}$$

where $\mathbf{u}$ is an arbitrary unit vector, and A and α' denote $A(\mathbf{q})$ and $\alpha'(\mathbf{q})$, respectively, which are the absolute value and the argument of the complex number $\tilde{J}_{12}(\mathbf{q})/J_1$; so that $\tilde{J}_{12}(\mathbf{q}) = J_1 A(\mathbf{q})\, e^{i\alpha'(\mathbf{q})}$. Then $\varepsilon = -2\lambda^{(+)}(\mathbf{q})$ and $\boldsymbol{\sigma}_{\mathbf{q}\nu}^{(+)}$ or $\varepsilon = -2\lambda^{(-)}(\mathbf{q})$ and $\boldsymbol{\sigma}_{\mathbf{q}\nu}^{(-)}$ correspond to the ground state according to whether J_1 is positive or negative.

Explicit forms of $\tilde{J}_{\mu\nu}(\mathbf{q})$ are given by

$$\tilde{J}_{11}(\mathbf{q}) = \tilde{J}_{22}(\mathbf{q}) = 2J_2[\cos q_x + \cos q_y + \cos(q_x - q_y)] \tag{3.10}$$

$$\begin{aligned}\tilde{J}_{12}(\mathbf{q}) = \tilde{J}_{21}^{*}(\mathbf{q}) &= J_1 A e^{i\alpha'} \\ &= \exp[-i(q_x + q_y)/3][J_1\{1 + \exp(iq_x) + \exp(iq_y)\} \\ &\quad + J_3\{\exp[i(q_x - q_y)] + \exp[i(-q_x + q_y)] \\ &\quad + \exp[i(q_x + q_y)]\}]\end{aligned} \tag{3.11}$$

where

$$\begin{aligned}\alpha' &= \alpha - (q_x + q_y)/3 \\ \cos\alpha &= \{1 + \cos q_x + \cos q_y + \zeta[2\cos(q_x - q_y) + \cos(q_x + q_y)]\}/A \\ \sin\alpha &= [\sin q_x + \sin q_y + \zeta \sin(q_x + q_y)]/A \\ A &= \{3 + 2[\cos q_x + \cos q_y + \cos(q_x - q_y)] \\ &\quad + \text{terms of order } \zeta \text{ and } \zeta^2\}^{1/2}\end{aligned} \tag{3.12}$$

and $q_x = \mathbf{q}\cdot\mathbf{a}_1$, $q_y = \mathbf{q}\cdot\mathbf{a}_2$, and $\zeta = J_3/J_1$. In terms of X and Y defined by (2.11), $\varepsilon = \mathscr{H}/N$ is expressed as follows:

$$\varepsilon = -4J_2(2Y^2 + 2XY - 1) \mp 2J_1 A \tag{3.13}$$

where

$$\begin{aligned}A = [&(4Y^2 + 4XY + 1) + \zeta^2(16Y^4 + 16X^2Y^2 - 24Y^2 - 8Y^2 + 9) \\ &+ 2\zeta(8XY^3 + 4Y^2 + 2X^2 - 2XY - 3)]^{1/2}\end{aligned} \tag{3.14}$$

The minimum of the energy is given by the upper sign when $J_1 > 0$ and the lower sign when $J_1 < 0$.

From the conditions $\partial\varepsilon/\partial q_x = \partial\varepsilon/\partial q_y = 0$, we have

$$\begin{aligned}\{&4J_2 Y + A^{-1}[8\zeta Y^3 + 16\zeta^2 XY^2 + (2 - 2\zeta)\, Y \\ &+ (4\zeta - 8\zeta^2)\, X]\}(1 - X^2)^{1/2} = 0\end{aligned} \tag{3.15}$$

$$\begin{aligned}\{&4J_2(X + 2Y) + A^{-1}[32\zeta^2 Y^3 + 24\zeta XY^2 + 16\zeta^2 YX^2 \\ &+ (4 - 24\zeta^2 + 8\zeta)\, Y + (2 - 2\zeta)\, X]\}(1 - Y^2)^{1/2} = 0\end{aligned} \tag{3.16}$$

First we consider the case $J_3=0$. Then (3.15), (3.16) have six solutions, A_+, A_-, B_+, B_-, C, and D, which are given in Table II. They are candidates of the ground state. The energy ε as a function of $\xi=J_1/J_2$ is shown in Fig. 11. We see that B_+, B_-, and C do not appear as a ground state, except at the points where they are degenerate with D. A_+ and A_- satisfy the strong constraint (3.5a). A_+ is the ferromagnetic state and A_- is the antiferromagnetic state. D is a helical state, as will be seen later. The phase diagram in the J_1–J_2 plane is shown in Fig. 12. In the case of the antiferromagnetic state, the situation is similar to the one for the systems on the triangular lattice.

In the region where D is the lowest energy state, we see that the energy is the same on the line

$$X=-Y+\left(\frac{\xi^2}{16}+\frac{1}{4}\right)\frac{1}{Y} \qquad (Y\neq 0) \tag{3.17}$$

and, when $Y=0$, X is arbitrary ($-1\leqslant X\leqslant 1$). Hence the wave number $\mathbf{q}$ for the lowest energy state cannot be determined. The infinite degeneracy is removed if we add an infinitesimal small third-neighbor interaction. Then (3.13) is transformed into

$$\varepsilon=\varepsilon_0+\varepsilon_1$$

Table II. Spin Configurations of the Systems on the Plane Hexagonal Lattice, and the Wave Number and the Energy

$$X_1=-Y_1+\left(\frac{\xi^2}{16}-\frac{1}{4}\right)\Big/Y_1 \quad (-1\leqslant Y_1\leqslant 1,\ Y_1\neq 0)$$

X_1 is arbitrary $\quad (-1\leqslant X_1\leqslant 1,\ Y_1=0)$

Type	(X, Y)	(q_x, q_y)	ϕ_{12}	Energy per unit cell
A_+	$(\pm 1, \pm 1)$	$(0, 0)$	0	$-6J_2(\xi+2)$ $(J_1>0)$
A_-	$(\pm 1, \pm 1)$	$(0, 0)$	π	$-6J_2(2-\xi)$ $(J_1<0)$
B_+	$(\pm 1, \mp 1)$	(π, π)	π	$2J_2(2-\xi)$ $(J_1>0)$
B_-	$(0, 0)$	$(\pi, 0)$	0	$2J_2(2+\xi)$ $(J_1<0)$
		$(0, \pi)$		
C	$\left(\pm 1, \mp\frac{1}{2}\right)$	$\left(\pm\frac{2}{3}\pi, \mp\frac{2}{3}\pi\right)$	0	$6J_2$
D	(X_1, Y_1)	Indefinite		$J_2(\xi^2+12)/2$ $(J_2<0,\ -6\leqslant\xi\leqslant 6)$

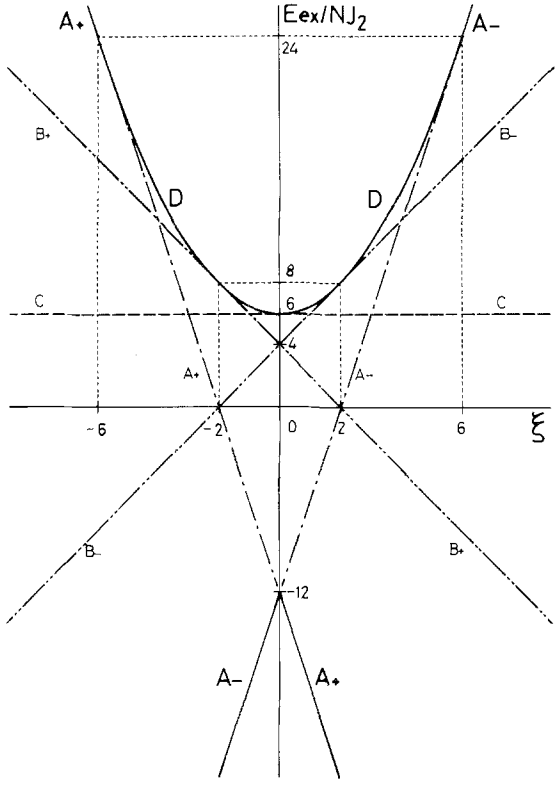

Fig. 11. ε/J_2 versus ξ for several states of the systems on the plane hexagonal lattice. Here E_{ex}/N denotes ε. The solid lines show the ground state.

where

$$\varepsilon_0 = -4J_2(2Y^2+2XY-1)-2|J_1|(4Y^2+4XY+1)^{1/2} \tag{3.18}$$

$$\varepsilon_1 = -\mathrm{sgn}(J_1)\,2J_3\frac{8XY^3+4Y^2+2X^2-2XY-3}{(4Y^2+4XY+1)^{1/2}} \tag{3.19}$$

ε_0 is a constant on the line given by (3.17). The spin configuration in the ground state is determined by minimizing ε_1. We substitute (3.17) into (3.19), and then $\partial\varepsilon_1/\partial Y=0$ gives

$$(32Y^2-\xi^2+4)(Y^2+\xi-2)(8Y^2-\xi-2)=0 \tag{3.20}$$

The three solutions of (3.20) are denoted by D_{1a}, D_{2a}, and D_{3a}. The restriction $-1\leqslant Y\leqslant 1$ gives allowable regions of ξ for each solution. The

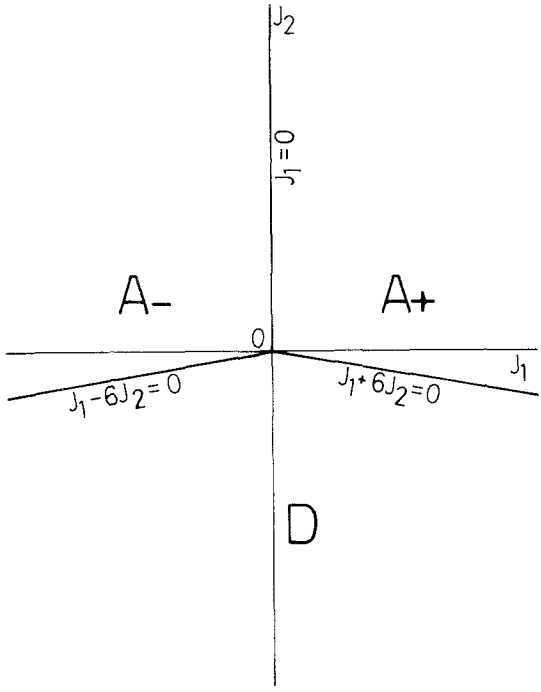

Fig. 12. Phase diagram of the classical Heisenberg and planar models on the plane hexagonal lattice of $J_3 = 0$.

least value of the energy is attained either by D_{1a}, D_{2a}, or D_{3a}, or at the zone edges. The latters are classified as D_{1b} $[X = \pm 1, Y \mp (\xi + 2)/4]$, D_{2b} $[X = \pm 1, Y = (\xi - 2)/4]$, and D_{3b} $[X = \pm(\xi^2 - 20)/16, Y = \pm 1]$. Allowable regions of ξ and the energies of D_{1b}, D_{2b}, and D_{3b} are the same as those of D_{1a}, D_{2a}, and D_{3a}. The value of ε_1/J_3 is shown as a function of ξ in Fig. 13. These situations are shown in Table III and in the Brillouin zone in Fig. 14.

Let the spin configurations of these solutions be

$$\begin{pmatrix} \mathbf{S}_{n1}^{(\pm)} \\ \mathbf{S}_{n2}^{(\pm)} \end{pmatrix} = \sum_{l=1}^{3} \begin{pmatrix} \mathbf{b}_{l1} \exp(i\mathbf{q}_l \cdot \mathbf{R}_{n1}) + \mathbf{b}_{l1}^* \exp(-i\mathbf{q}_l \cdot \mathbf{R}_{n1}) \\ \mathbf{b}_{l2} \exp(i\mathbf{q}_l \cdot \mathbf{R}_{n2}) + \mathbf{b}_{l2}^* \exp(-i\mathbf{q}_1 \cdot \mathbf{R}_{n2}) \end{pmatrix} \tag{3.21}$$

$$\mathbf{b}_{l1} = \boldsymbol{\sigma}_{\mathbf{q}_l 1}, \qquad \mathbf{b}_{l2} = \pm \boldsymbol{\sigma}_{\mathbf{q}_l 1} \exp[i\alpha'(\mathbf{q})] \tag{3.22}$$

where the upper and lower signs in (3.22) correspond to $J_1 < 0$ and $J_1 > 0$, respectively. $\mathbf{q}_l$ for $l = 1, 2$, and 3 are given in Table III; for example, $\mathbf{q}_1 = (2Q_1, Q_1)$, $\mathbf{q}_2 = (Q_1, 2Q_1)$, and $\mathbf{q}_3 = (Q_1, -Q_1)$ in D_1. By similar considerations to those given for the systems on the triangular lattice, we see

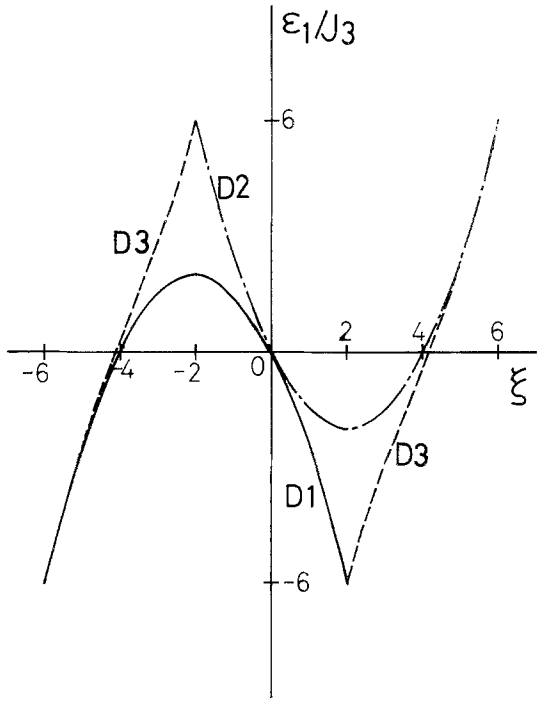

Fig. 13. ε_1/J_3 versus ξ. The solid, dash-dotted, and dashed lines denote the states D_1, D_2, and D_3, respectively.

that $\mathbf{b}_{l1}$ does not vanish for only one of l when the strong constraint (3.5a) is imposed. Then if $\mathbf{b}_{11} \neq 0$, the spin configuration is given by

$$\mathbf{b}_{11} = (\mathbf{u}_1 - i\mathbf{v}_1)/2$$

$$\begin{aligned}\begin{pmatrix}\mathbf{S}_{n1}\\ \mathbf{S}_{n2}\end{pmatrix} &= \begin{pmatrix}\tfrac{1}{2}(\mathbf{u}_1 - i\mathbf{v}_1)\exp(i\mathbf{q}\cdot\mathbf{R}_{n1})\\ \pm\tfrac{1}{2}(\mathbf{u}_1 - i\mathbf{v}_1)\exp(i\alpha' + i\mathbf{q}\cdot\mathbf{R}_{n2})\end{pmatrix}\\ &\quad + \begin{pmatrix}\tfrac{1}{2}(\mathbf{u}_1 + i\mathbf{v}_1)\exp(i\mathbf{q}\cdot\mathbf{R}_{n1})\\ \pm\tfrac{1}{2}(\mathbf{u}_1 + i\mathbf{v}_1)\exp(i\alpha' + i\mathbf{q}\cdot\mathbf{R}_{n2})\end{pmatrix}\\ &= \begin{pmatrix}\mathbf{u}_1\\ \mathbf{u}_2\end{pmatrix}\cos\mathbf{q}\cdot\mathbf{R}_{n1} + \begin{pmatrix}\mathbf{v}_1\\ \mathbf{v}_2\end{pmatrix}\sin\mathbf{q}\cdot\mathbf{R}_{n1} \qquad (3.23)\end{aligned}$$

$$\begin{pmatrix}\mathbf{u}_2\\ \mathbf{v}_2\end{pmatrix} = \pm\begin{pmatrix}\cos\alpha & \sin\alpha\\ -\sin\alpha & \cos\alpha\end{pmatrix}\begin{pmatrix}\mathbf{u}_1\\ \mathbf{v}_1\end{pmatrix} \qquad (3.24)$$

where $\mathbf{u}_\nu$ and $\mathbf{v}_\nu$ ($\nu = 1, 2$) stand for $\mathbf{u}_{\mathbf{q}\nu}$ and $\mathbf{v}_{\mathbf{q}\nu}$ ($\nu = 1, 2$) which are such orthogonal unit vectors that $(\mathbf{u}_{\mathbf{q}1}, \mathbf{v}_{\mathbf{q}1})$ and $(\mathbf{u}_{\mathbf{q}2}, \mathbf{v}_{\mathbf{q}2})$ lie in the same plane,

Table III. Spin Configurations of the Systems on the Plane Hexagonal Lattice with Interactions up to Third Neighbors

$$X_1 = X_2 = X_3 = -Y + (\xi^2/16 - 1/4)/Y \quad Q_1 = \cos^{-1}[-(\xi+2)/4]$$
$$Q_2 = \cos^{-1}[(\xi-2)/4] \quad Q_3 = \cos^{-1}[(\xi^2-20)/16]$$
$$\psi_1 = \mathrm{sgn}(J_3)\,|\cos^{-1}[2(\cos Q_3 + 2)/\xi]| + \pi$$
$$\psi_2 = \mathrm{sgn}(J_3)\,|\cos^{-1}[2(2\cos Q_3 + 1)/\xi]| + \pi$$

Type	(X, Y)	(q_x, q_y)	ϕ_{12}	ε_1
D_{1a}	$\left(X_1, \pm\frac{1}{2}\left(1-\frac{\xi}{2}\right)^{1/2}\right)$	$(2Q_1, Q_1)$	Q_1	$-J_3\xi(\xi+4)/2$
		$(Q_1, 2Q_1)$		$(-6 \leqslant \xi \leqslant 2)$
D_{1b}	$\left(\pm 1, \mp\frac{1}{4}(\xi+2)\right)$	$(Q_1, -Q_1)$	0	
D_{2a}	$\left(X_2, \pm\frac{1}{2}\left(1+\frac{\xi}{2}\right)^{1/2}\right)$	$(2Q_2, Q_2)$	$Q_2+\pi$	$J_3\xi(\xi-4)/2$
		$(Q_2, 2Q_2)$		$(-2 \leqslant \xi \leqslant 6)$
D_{2b}	$\left(\pm 1, \pm\frac{1}{4}(\xi-2)\right)$	$(Q_2, -Q_2)$	π	
D_{3a}	$\left(X_3, \pm\frac{1}{4}\left(\frac{\xi^2}{2}-2\right)^{1/2}\right)$	$(Q_3, 0)$	ψ_1	$J_3(\xi^4+8\xi^2-432)/32\xi$
		$(0, Q_3)$		$(-6 \leqslant \xi \leqslant -2, 2 \leqslant \xi \leqslant 6)$
D_{3b}	$\left(\pm\frac{1}{16}(\xi^2-20), \pm 1\right)$	(Q_3, Q_3)	ψ_2	

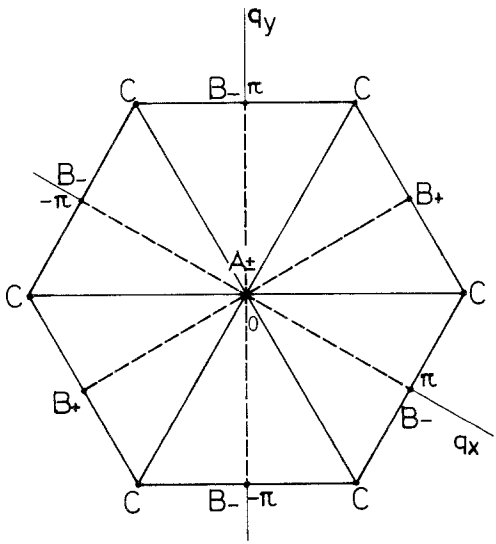

Fig. 14. The first Brillouin zone of the plane hexagonal lattice. The origins are A_+ and A_-. The solid and dashed lines, respectively, denote D_1 and D_3 in the case of $J_3 > 0$ and D_2 and D_3 in the case of $J_3 < 0$.

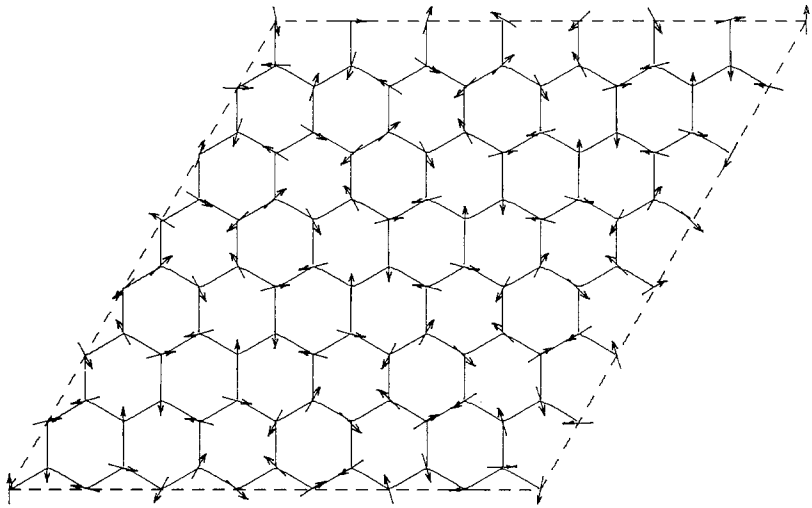

Fig. 15. Spin configuration of the systems on the plane hexagonal lattice. State D_3, where $J_1/J_2 = 4$, $\mathbf{q} = (0.577\pi, 0.577\pi)$, $\phi_{12} = 256°$, $J_3 > 0$.

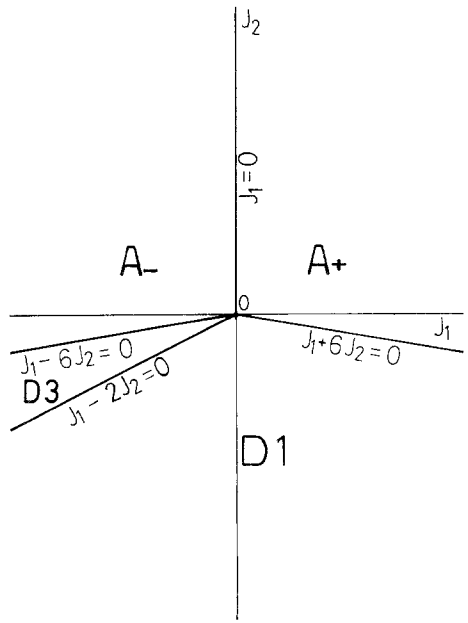

Fig. 16. Phase diagram of the classical Heisenberg and planar models on the plane hexagonal lattice, in the case of $J_3 > 0$. The replacements $J_1 \to -J_1$, $A_+ \to A_-$, $A_- \to A_+$, and $D_1 \to D_2$ give the one for the case of $J_3 < 0$.

and the sense of the rotation in going from $\mathbf{u}_{q1}$ to $\mathbf{v}_{q1}$ is the same as that from $\mathbf{u}_{q2}$ to $\mathbf{v}_{q2}$; so that, $\mathbf{u}_{q1}\times\mathbf{v}_{q1}=\mathbf{u}_{q2}\times\mathbf{v}_{q2}$. The relative phase angle ϕ_{12} from $\mathbf{S}_{n1}$ to $\mathbf{S}_{n2}$ is determined by

$$\phi_{12}=\alpha \quad \text{for} \quad J_1<0 \quad \text{and} \quad \alpha+\pi \quad \text{for} \quad J_1>0 \tag{3.25}$$

where α is given in (3.12). Hence the spin configuration of the system in which the signs of J_1 and J_3 are changed at the same time is simply reduced from that of the original system by reversing the directions of spins on one sublattice ($\mathbf{S}_{m1}\to\mathbf{S}_{m1}$, $\mathbf{S}_{m2}\to-\mathbf{S}_{m2}$). When $\xi=0$, the state C is realized. C is a superposition of two independent triangular states T for two triangular sublattices $\nu=1$ and 2.

Thus we confirm that D_1, D_2, and D_3 are three kinds of helical states. D is divided into D_1 and D_3 when $J_3>0$, and into D_2 and D_3 when $J_3<0$. Examples of the spin configurations are shown in Fig. 15. As mentioned in the case of the triangular lattice, each spin pattern is understood as drawn in the $\mathbf{u}_q$–$\mathbf{v}_q$ plane associated to each lattice point. In the case of the classical planar model, the $\mathbf{u}_q$–$\mathbf{v}_q$ plane coincides with the x–y plane. The phase diagram in the J_1–J_2 plane is shown in Fig. 16. It is compared with the one for the corresponding Ising model[2] shown in Fig. 17. The

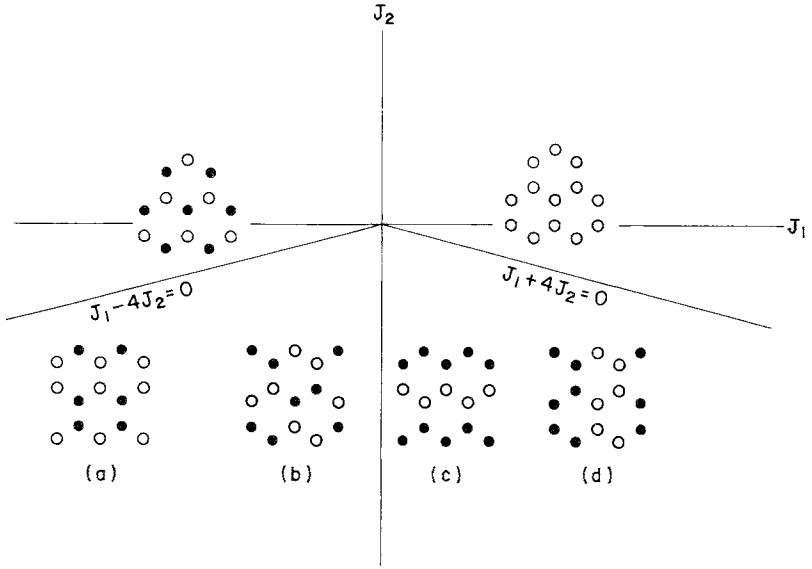

Fig. 17. Phase diagram of the Ising model on the plane hexagonal lattice. (a) and (b) in the case of $J_1<0$, and (c) and (d) in the case of $J_1>0$. They are degenerate in the respective regions.

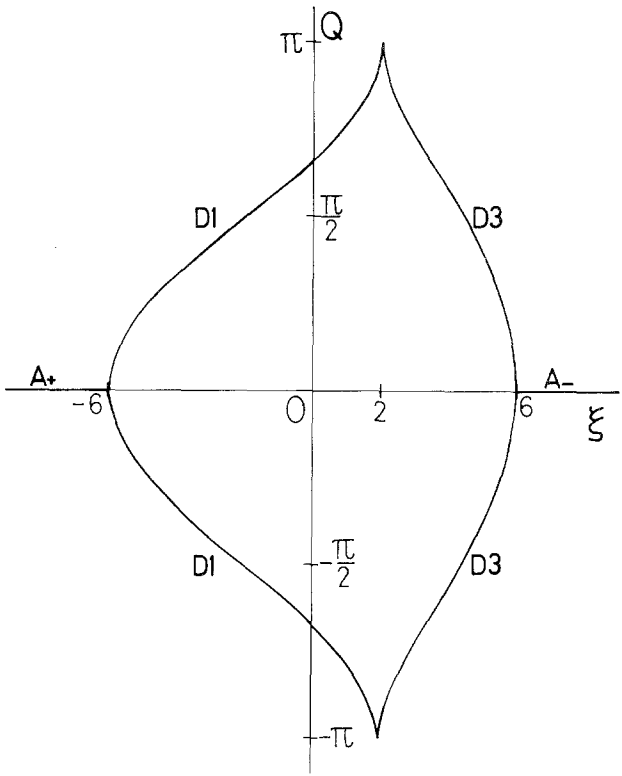

Fig. 18. A component Q of $\mathbf{q}$ versus ξ, showing the change of the wave vector $\mathbf{q}$ against the ratio of the exchange interactions for the systems on the plane hexagonal lattice in the case of $J_3 > 0$.

variation of the wave vector is shown as a function of $\xi = J_1/J_2$ in Fig. 18, which shows the transitions $A_+ \to D_1 \to D_3 \to A_-$ as J_1 decreases from plus infinity to minus infinity for a fixed negative J_2.

4. CONCLUSION AND DISCUSSION

In this paper the energy and the spin configuration of the classical Heisenberg and classical planar models on the triangular and plane hexagonal lattices were determined.

In the case of the Ising model, complex structures appear especially under a magnetic field. The energies of these states, however, are higher than that of the triangular state, for the present systems. We saw that the ground state energy is obtained within the single $\mathbf{q}$ scheme in the present

case; though we have to consider the degeneracy of the states in order to get the spin configurations of the ground state.

In the systems on the triangular lattice with first- and second-neighbor interactions, the boundaries between the ferromagnetic, antiferromagnetic, triangular, and two helical phases were obtained. The triangular phase of the classical planar model on the triangular lattice is doubly degenerate, and the chirality order exists.[8,9]

In the systems on the plane hexagonal lattice with the first- and second-neighbor interactions, there exist some regions in the J_1–J_2 plane, where there occur an infinite number of $\mathbf{q}$ giving the ground state energy, and an infinistesimal third-neighbor interaction removes the infinite degeneracy. Then the phase diagram was obtained by introducing a positive or negative infinitesimal J_3. Kanamori *et al.*[10] found complex ground state spin configurations of the Ising model on the hexagonal lattice in some region of the J_1/h–J_2/h plane, where h is the magnitude of the external field. The energy of it is higher than the ground state energy of the present model, and similar configurations are not realized in our model at zero external field.

Up to this point we considered the two-dimensional triangular and plane hexagonal lattices. Low-dimensional substances in experiments are not purely two-dimensional but have layered structures. In such cases they have longitudinal exchange interactions. If the longitudinal interactions are restricted only within the same chain, the whole spin configuration is simply an accumulation of a single surface configuration with $q_z = 0$ or π according as $J_0 > 0$ or $J_0 < 0$, where J_0 is the coefficient of the interaction. When a second-neighbor interaction in the x–z (or y–z, etc.) plane exists, complex spin configurations other than these will appear.

Many of the low-dimensional substances in experiments are analyzed[11] in terms of the Ising model. They are, however, neither pure Ising nor pure classical Heisenberg or planar model. The ground states of the intermediate models, i.e., the Ising–Heisenberg or Heisenberg–XY model will be investigated in the future.

ACKNOWLEDGMENTS

The authors acknowledge helpful discussions with Professor S. Inawashiro, Dr. S. Fujiki, and Dr. S. Miyashita.

REFERENCES

1. M. Kaburagi and J. Kanamori, *J. Appl. Phys. Suppl.* **2**(Pt. 2):145 (1974); Y. Tanaka and N. Uryû, *J. Phys. Soc. Japan* **39**:825 (1975) (see Fig. 3).

2. T. Kudō and S. Katsura, *Prog. Theor. Phys.* **56**:435 (1976).
3. A. Yoshimori, *J. Phys. Soc. Japan* **14**:807 (1959).
4. D. H. Lyons and T. A. Kaplan, *Phys. Rev.* **120**:1580 (1960); see also J. M. Luttinger, and L. Tisza, *Phys. Rev.* **70**:954 (1946); J. M. Sanchez, D. Gratias, and D. de Fontaine, *Acta Crystallogr. A* **38**:214 (1982).
5. T. Nagamiya, *Solid State Physics*, Vol. 20, F. Seitz and D. Turnbull, eds., p. 305, Academic Press, New York (1967).
6. Y. Yamamoto and T. Nagamiya, *J. Phys. Soc. Japan* **32**:1248 (1972); T. Akino and K. Motizuki, *J. Phys. Soc. Japan* **31**:691 (1971).
7. D. H. Lee, R. G. Gaflish, J. D. Joanopoulos, and F. Y. Wu, *Phys. Rev. B* **29**:2680 (1984); D. H. Lee, J. D. Joanopoulos, J. W. Negele, and D. P. Landau, *Phys. Rev. Lett.* **52**:433 (1984); Vik. S. Dotsenko and G. V. Uimin, *Zh. Eksp. Teor. Fiz.* **40**:236 (1984) [*Sov. Phys. JETP Lett.* **40**:1009 (1985)].
8. J. Villain, *J. Phys. C* **10**:1717, 4793 (1977).
9. S. Miyashita and H. Shiba, *J. Phys. Soc. Japan* **53**:1145 (1984).
10. J. Kanamori, *J. Phys. Soc. Japan* **53**:250 (1984); M. Kaburagi, T. Tonegawa, and J. Kanamori, *J. Phys. Soc. Japan* **53**:1971 (1984).
11. M. Mekata and K. Adachi, *J. Phys. Soc. Japan* **44**:806 (1978); K. Hirakawa, H. Kadowaki, and K. Ubukoshi, *J. Phys. Soc. Japan* **52**:1814 (1983); H. Kawamura and S. Miyashita, *J. Phys. Soc. Japan* **53**:9 (1984); S. Fujiki, K. Shutoh, and S. Katsura, *J. Phys. Soc. Japan* **53**:1371 (1984).